Dust Removal Technolgy for a Mars In Situ Resource Utilization System

C.I. Calle[1], M.R. Johansen[2], B.S. Williams[3], M.D. Hogue[4] P.J. Mackey[5] and J.S. Clements[6]

[1,2,4,5] *Electrostatics and Surface Physics Laboratory, NASA, Kennedy Space Center, FL 32899*
[3] *University of South Alabama, Mobile, AL 36688*
[6] *Department of Physics and Astronomy, Appalachian State University, Boone, NC 28608*

Several In Situ Resource Utilization (ISRU) systems being considered to enable future manned exploration of Mars require capture of Martian atmospheric gas to extract oxygen and other commodities. However, the Martian atmosphere contains relatively large amounts of dust which must be removed in the collection systems of the ISRU chambers. The amount of atmospheric dust varies largely with the presence of daily dust devils and the less frequent but much more powerful global dust storms. A common and mature dust removal technology for terrestrial systems is the electrostatic precipitator. With this technology, dust particles being captured are imparted an electrostatic charge by means of a corona discharge. Charged dust particles are then driven to a region of high electric field which forces the particles onto a collector for capture. Several difficulties appear when this technology is adapted to the Martian atmospheric environment. At the low atmospheric pressure of Mars, electrical breakdown occurs at much lower voltages than on Earth and corona discharge is difficult to sustain. In this paper, we report on our efforts to obtain a steady corona/glow discharge in a simulated Martian atmosphere of carbon dioxide at 9 millibars of pressure. We also present results on the design of a dust capture system under these atmospheric conditions.

Nomenclature

a	=	electrode radius
a_0	=	particle radius
b	=	ion mobility
d	=	electrode gap distance
E	=	electric field generated by the potential difference across precipitator electrodes
I	=	ion current
k	=	Boltzmann's constant
L	=	cylinder length
R	=	cylinder radius
r	=	ion distance from high voltage electrode
T	=	temperature of the gas in Kelvin
N_0	=	ion number density
c	=	mean ion velocity
V	=	Potential difference between electrodes
ε_0	=	permittivity of free space
κ	=	relative permittivity of the particle

---

[1] Senior Resrarch Physicist, Electrostatics and Surface Physics Laboratory, NE-S-1, NASA Kennedy Spece Center.
[2] Co-Op Student, Electrostatics and Surface Physics Laboratory, NE-S-1, NASA Kennedy Spece Center.
[3] Student, Aerospace Engineering, University of South Alabama, Mobile
[4] Physicist, Electrostatics and Surface Physics Laboratory, NE-S-1, NASA Kennedy Spece Center.
[5] Physicist, Electrostatics and Surface Physics Laboratory, NE-S-1, NASA Kennedy Spece Center.
[6] Professor, Dept. of Physics and Astronomy, Appalachian State University, Boone, NC.

I. Introduction

THE human exploration of Mars will make extensive use of local resources for the production of consumables. One important resource is the Martian atmosphere itself, which may yield oxygen, methane, and water. However, the ever-present dust in the Martian atmospheric gas must be removed from the intakes bringing it to the processing chambers and ovens before these systems can perform their extraction of these commodities.

Dust removal from a gaseous flow can be accomplished in different ways. The most common approaches for terrestrial applications are fabric filters and electrostatic precipitators. The low pressure of the Martian atmosphere, at 7 to 10 mbars, presents difficult challenges to both of these techniques. Fabric filters have a pressure drop and, at the low Mars pressures, would make the use of a vacuum pump downstream inpractical. Using upstream compression would compensate for the pressure drop, but the abrasiveness of the Martian dust present in the gas may damage the compressor. And while the pressure drop in not an issue with an electrostatic precipitator, the low atmospheric pressure on Mars prevents the establishment of the large electrostatic potential differences required for this technology.

We report here on our efforts to design and test an electrostatic precipitator system that could work under the challenging conditions imposed by the Martian atmosphere. We include results of experiments performed at simulated Martian atmospheric composition and pressure as well as preliminary efficiency results.

II. Electrical Properties of the Martian Atmosphere

With an atmospheric pressure between 7 to 10 mbars, the Martian atmosphere severly limits the potentials that can be applied to the electrodes of an electrostatic precipitator. An electrostatic precipitator collects dust particles that have been electrostatically charged by driving these charged dust particles onto one of the electrodes by means of an applied electric field. At 7-10 mbars, Townsend breakdown occurs ar relatively low potentials.[1] In Townsend avalanche breakdown, a cosmic ray particle can knock off an electron from the cathode of the precipitator or from a gas molecule. As this electron is accelerated in the applied electric field, it ionizes another gas molecule, thus releasing a second electron. These two electrons accelerated in the precipitator field can ionize additional gas molecules, creating an avalanche of electrons toward the anode. The positive ions created by the collisions with the electrons accelerate toward the cathode, where they release secondary electrons that can create a new cycle of avalanches.

In a weak electric field, the number of charges that are formed decreases and the electrons and ions recombine. If the field is strong, the number of charges increases and the avalanches increase, filling the entire space between the electrodes with ions, producing a breakdown.

The breakdown potential in Townsend breakdown in a uniform electric field depends on the product of the gap length d and the gas number density. This relationship is known as Paschen's law.[2] Historically, the gas pressure p is used instead of the number density. We performed experiments with a premixed gas to emulate the Martian atmosphere, composed of a mixture of 95% CO_2, 2.7% N_2, 1.6% A, 0.13% O_2, and 0.07% CO.[3] Data was taken at pressures ranging from 270 mbars to 466 mbars (200 mtorr to 350 torr) with gaps of 5 mm, 7.5 mm, and 10 mm. The low pressure data (Fig. 1) shows that breakdown potentials in CO_2 and in the Martian gas mixture are extremely similar. It appears as if CO_2 dictates the Paschen breakdown and that the other gases, present in relatively low concentrations, do not affect it substantially. The Martian gas breakdown voltages are equal to or slightly smaller than the CO_2 voltages by an average of 15 volts, perhaps due to the known lower breakdown potentials of nitrogen and argon, present in smaller concentrations. Based on these results, we used a 95% CO_2/5% humid air mixture to approximate the Martian atmosphere for this study as well as a 100% CO_2 atmosphere. Table 1 shows the breakdown potentials measured for selected gap distances in a carbon dioxide atmosphere at 9 mbars of pressure.

Table 1. Breakdown potentials for several gap distances in CO_2 at 10 mbars.[3]

Gap separation d (mm)	Breakdown Potential (V)
5	725
7.5	800
10	895
100	2800

Dust particle charging and migration are also affected by the low Martian atmospheric pressure. At 9 mbars, the mean free path of carbon dioxide molecules is about 4 μm, or about 100 times larger than at one atmosphere. Three charging regimes are defined based on the ratio of the molecular mean free path and the particle radius (Knudsen number): the continuum, free molecular, and transitional regimes. On Mars, dust particle charging shifts to the transitional regime.

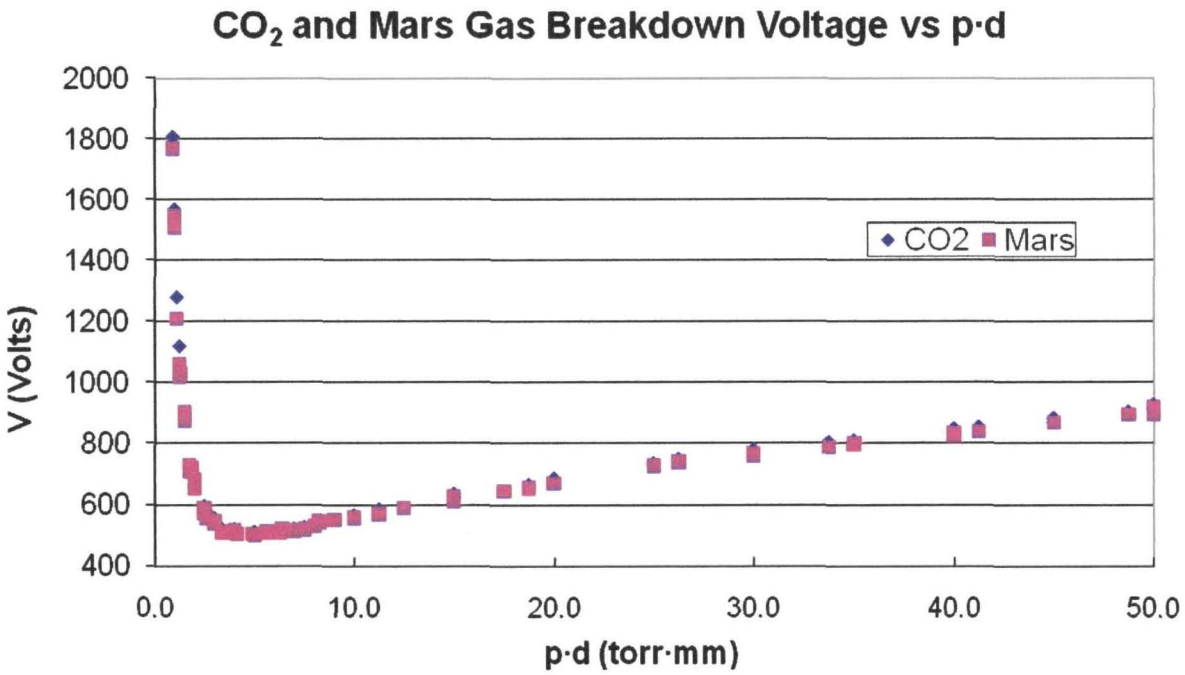

Figure 1. Paschen breakdown potentials versus pressure×distance for a Martian gas mixture (red squares) and for CO_2 (blue triangles)[3].

III. Precipitator Physics

An electrostatic precipitator consists of two electrodes set at an electrostatic potential difference that can drive charged particles to one of the electrodes for collection. There are two general types of electrostatic precipitators: Single-stage precipitators, where particle charging and particle collection take place in a single state; and two-stage precipitators, with a pre-charging stage and a collecting stage. In both precipitator types, dust particles are charged using corona generation around the high voltage discharge electrode, which ionizes gas molecules. These ions are accelerated by the electric field E in the region between the electrodes, but numerous collisions with gas molecules results in a constant drift velocity characterized by an ion mobility b = velocity/E. The ions transfer charge to dust particles encountered in their path as they drift to the grounded collecting electrode. The ions form space charge which modifies the applied E between the electrodes. The electric field for a wire-cylinder geometry without space charge is given by:

$$E(r) = \frac{V}{r \ln\left(\frac{R}{a}\right)} \tag{1}$$

where V is the applied voltage, r is the distance from the wire, a is the wire radius, and R is the cylinder radius. The expression for the case with space charge is:[4]

$$E(r) = \sqrt{\frac{I}{2\pi\varepsilon_0 Lb} + \left(\frac{a}{r}\right)^2 \left\{\left(\frac{V}{a \ln\frac{R}{a}}\right)^2 - \frac{I}{2\pi\varepsilon_0 Lb}\right\}} \tag{2}$$

where I is the ion current, L is the length of the wire-cylinder, and b is the ion mobility. Larger ion currents yield more space charge, substantially increasing the applied electric field.

Ions accelerated in this electric field charge dust particles in two distinct ways: field charging and diffusion charging. In field charging, ions are driven by the electric field and collide with dust particles. The probability of ion adhesion to dust particles is proportional to the square of the particle radius. This charging process stops when dust particle charge saturation is reached.

In diffusion charging, thermal motion of gas ions causes random collisions with dust particles. In theory, diffusion charging does not reach saturation, because there is always a finite probability of an ion with a high enough kinetic energy to overcome the potential barrier of the charged particle. The expressions for the saturation and diffusion charges, discussed in an earlier paper,[5] are:

$$Q_s = 12\pi\varepsilon_0 \frac{\kappa}{\kappa+2} a_0^2 E \tag{3}$$

and

$$q(t) = \frac{4\pi\varepsilon_0 kT}{e} \ln\left(\frac{a_0 N_0 e^2 c_i t}{4\varepsilon_0 kT} + 1\right) \tag{4}$$

where ε_0 is the permittivity of free space, κ is the relative permittivity of the particle, a_0 is the particle radius, k is Boltzmann's constant, T is the temperature of the gas in Kelvin, N_0 is the ion number density, and c_i is the mean ion velocity. The term $\kappa/(\kappa+2) = 1$ for conductive particles.

IV. Dust in the Martian Atmosphere

The surface of Mars is covered with dust with a similar composition and size throughout the planet due to its constant redistribution during global dust storms and dust devils. These dust storms and dust devils uplift dust into the rarefied atmosphere.

Calculations based on optical instrumentation on spacecraft in orbit around Mars and on rovers on the surface have yielded estimates for the average diameter of dust particles in the atmosphere. Using this data, Landis *et al* believe that Martian atmospheric dust has a three-component particle size distribution: *Atmospheric dust* suspended for long periods of time, with radii ranging from 1 to 2 μm, with an average value of 1.5 ± 0.2 μm; *settled dust*, raised into the atmosphere by wind and dust devils, with a radii under 5 μm; and *saltating particles*, with radii greater than 40 μm.[6]

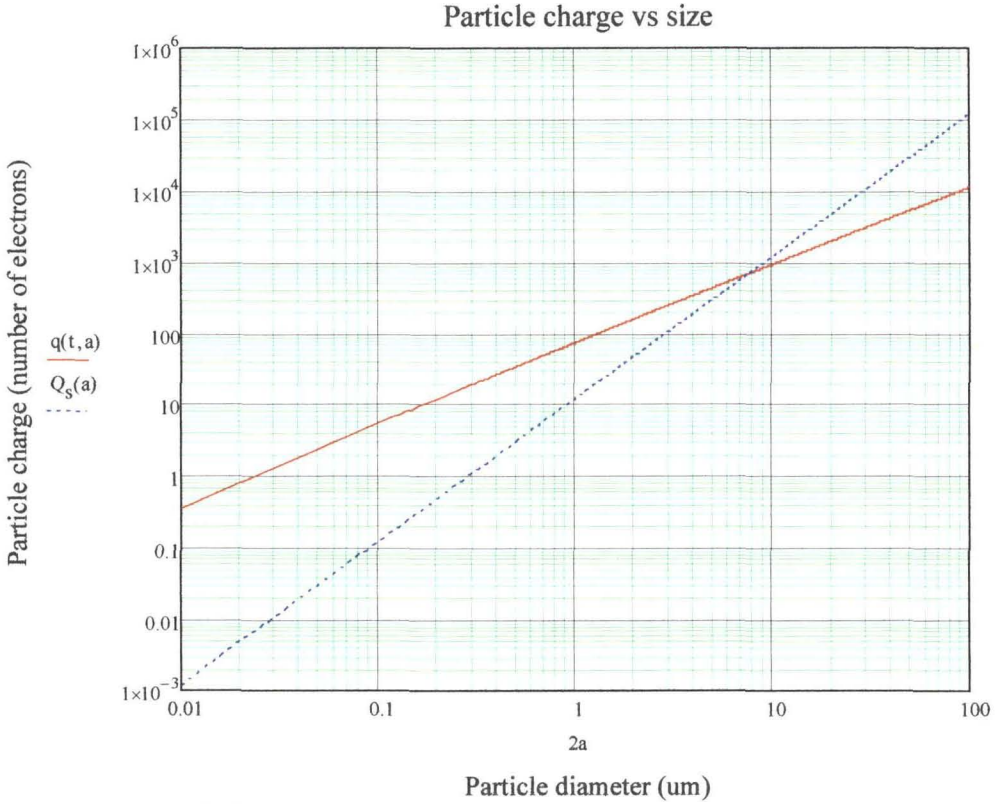

Figure 2. Continuum regime field saturation charge (dotted line) and diffusion charge (red line) for particles in CO_2 at 9 mbars with E = 0.23 kV/cm and an exposure time of 10s, as given by equations (3) and (4).

At 10 mbars of pressure, with a cylindrical electrostatic precipitator containing a 100 μm wire high voltage electrode and a 7.1-cm cylinder collecting electrode, the electric field halfway between these electrodes is 0.23 kV/cm. Under these conditions, field charging dominates for large particle sizes and short exposure times. For the

particles with diameters in the 2 to 10 μm range encountered in the Martian atmosphere, both field and diffusion charging contribute to the charging mechanism, with field charging contributing more to the larger 4 to 10 μm particles uplifted into the atmosphere during dust storm and dust devil activity, and both mechanisms contributing to the 2 to 4 μm particles normally found in the atmosphere (Fig. 2). Continuum regime theory only provides an order of magnitude estimate because, as we stated earlier, transitional regime theory is more appropriate for this particle size range at Mars gas pressures. In fact, the longer mean free paths at the low Mars pressures may shift the dominant diffusion charging size range to larger dust particles. Unfortunately, transitional regime theory is quite complicated and several different ones requiring numerical solution have been proposed in the literature.[7-10]

V. Experiments

A. Electrostatic Precipitator Current-Voltage Characteristics

Three 30-cm long cylinders with inner diameters of 5.2 cm, 7.1 cm, and 9.5 cm, a 0.3-cm rod, and two wires with 70 μm and 100 μm in diameter were used for the outer and inner electrodes of the precipitator. All 9 combinations were tested in a vacuum chamber evacuated to 9 mbars of carbon dioxide pressure.

We obtained current-voltage (*I-V*) curves for seven geometries at 9 mbars in CO_2 and in 95% CO_2-5% air mixture, to approximate more closely the Martian atmospheric composition (Fig. 3). With the *I-V* curves, voltages for corona onset and streamer corona were determined. The data for the 0.3 cm rod emphasizes how different the corona discharge is at low pressures compared to one atmosphere. In contrast to the atmospheric pressure case, corona current was easily obtained at low voltages using this large diameter rod and also for a very large 1.26 cm rod (not shown).

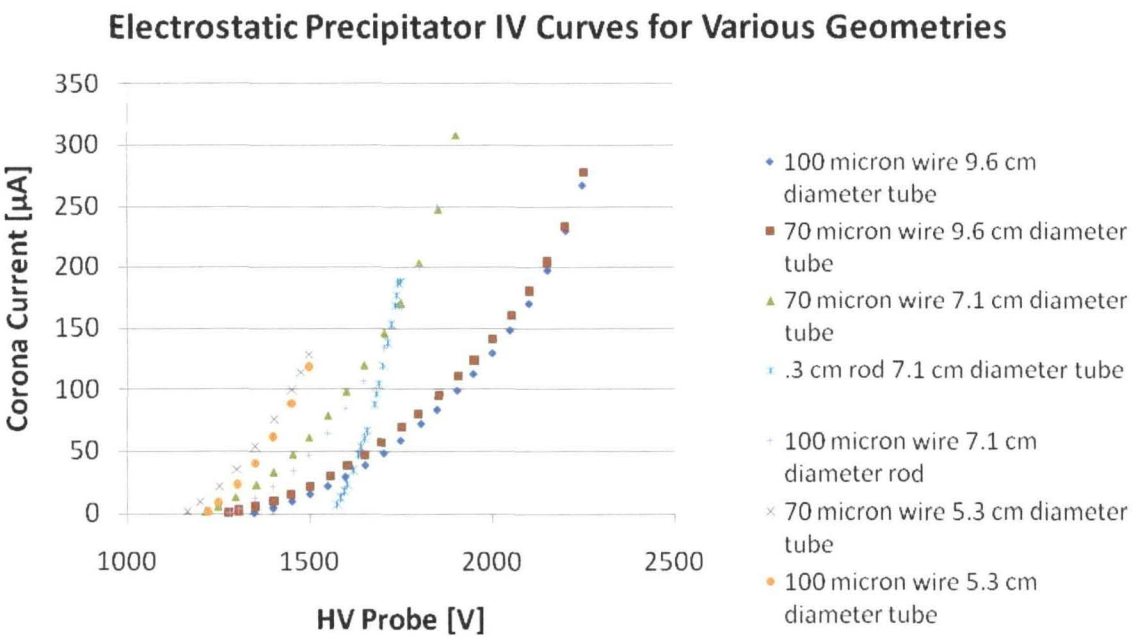

Figure 3. Current-Voltage (*I-V*) curves for seven configurations of the precipitator. Data taken with clean electrodes and positive polarity at 9 mbar in CO_2.

B. Corona Charging Experiments

To test the charging performance of the precipitator geometry in the continuum regime, where field charging theory clearly applies, we performed experiments with three large brass spheres. The spheres, with diameters of 0.47 cm, 0.95 cm and 1.27 cm, were lowered halfway into the precipitator—away from distorted edge fields—with a thin insulating Teflon thread. Then the corona discharge was turned on for 10 seconds using a DC high voltage supply. The power supply was then turned off and the charged sphere was lowered into a shielded Faraday cup. The Faraday cup was connected through a coaxial vacuum feed-through to an electrometer to obtain the value of the charge acquired by the sphere. The zero check on the electrometer was not deactivated until several seconds after the high

voltage was turned off to prevent stray ions from the corona from influencing the reading. In addition, the reading was not recorded until the sphere was raised out of the faraday cup so that the charge on the thread was not recorded. The conductive sphere was discharged when it touched the Faraday cup, which enabled the test to be repeated by simply raising the sphere back to the charging position inside the precipitator.

Figs. 4 and 5 show the ball charge data in 95% CO_2-5% humid air at 9 mbars for the 9.6-cm cylinder with 100-μm wire. In Fig. 4, the charge varies linearly with E as predicted by Eq. (3): a linear best fit line is shown for each data series. All the plots should extend through the origin as E is decreased because there is no field charging at zero E, and diffusion charging is predicted to be 1000× lower in this size range. However, the larger sphere sizes have an unexpected charge offset. Fig. 5 has a plot of charge vs. the ball diameter fit with a power law. At E = 0.11 kV/cm, the charge varies with the square of the diameter, as predicted by field theory. At the higher E field, the plot varies approximately with the square of the diameter (the 1.8 power instead of 2).

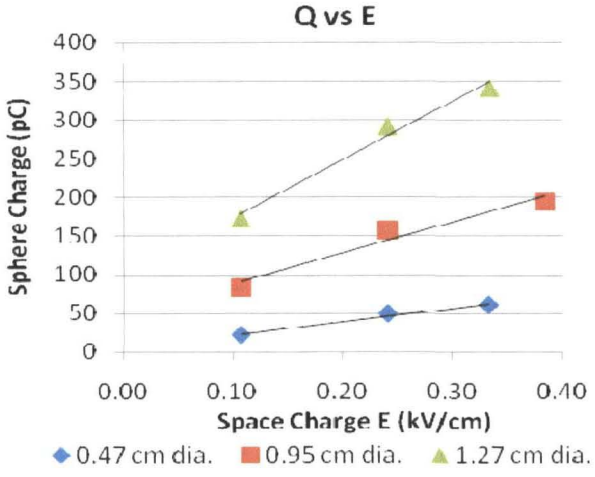

Figure 4. Experimental values of the average charge on 0.47, 0.95 and 1.27 cm diameter brass spheres vs. E.

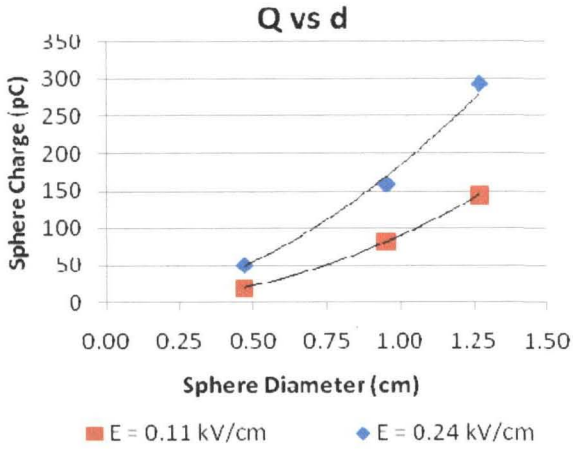

Figure 5. Experimental charge vs. sphere diameter for E fields of 0.11 and 0.24 kV/cm.

C. Precipitator Dust Collecting Experiments at Simulated Martian Conditions

The I-V curves for the seven configurations shown in Fig. 3 indicate that both the 100 μm and the 70 μm wires with the 9.6 cm diameter tube provide the largest stable voltage range between corona onset and streamer formation, as well as a relatively wide range in the corona current available for particle charging. Since the 100 μm wire is easier to handle, we decided to start our precipitator experiments with that configuration. However, the 9.6 cm width of the tube is perhaps too large for the comparatively small potentials allowed at the low pressure in the chamber. Dust particles falling through the precipitator have a larger distance to travel to the collecting electrode, resulting in little collection. Since the 100 μm wire with the 7.1-cm diameter tube did charge the simulant dust particles, our intial experiments were performed with that configuration.

About 5 mg of JSC Mars-1 simulant dust particles under 35 μm in diameter were introduced into the chamber through a Tygon tube and gas feed-through. The dust was aerosolized into a 1 liter polyethylene container inside the vacuum chamber located 1 cm above the ESP with a puff of CO_2 gas that raised the pressure in the chamber from 8.5 mbar to 9.3 mbar. A small net gas flow entered the ESP which carried dust through the precipitator, and the dust also fell with a terminal velocity dependent on the strength of gravity and the drag force. The dust collected on a silicon wafer mirror placed 5 cm under the exit of the ESP. Tribocharging of the dust during injection with no field on was measured with a Faraday cup located below the ESP. Appropriate tube and container material selection minimized this charging process to obtain a more controlled charging process in the precipitator.

Optical microscope images of the dust collected on the wafer with and without the precipitator fields turned on were taken to obtain particle size distributions and particle counts.[5] However, since the amount of dust entering the precipitator could not be controlled with our experimental set up, and since some of the simulant dust stays in the tubing and the jar and a fraction of the aerosolized dust falls outside the precipitator, efficiency determinations could not be performed with the optical method.

Since the 0.3 cm in diameter rod was even easier to handle, we also performed experiments with this electrode and the 7.1-cm tube. This configuration would facilitate precipitator maintenance procedures, since it is easier to assemble. It also allows higher electric fields to be applied without breakdown, which increases dust charging and

collection. Experiments with this geometry were also performed in CO_2 at 9 mbars. To test the upper limit of what this configuration could collect, we introduced about 12 mg of simulant containing dust particles under 35 μm in diameter. The aerosolized simulant dust passing through the precipitator and not driven to the collecting electrode by the electric field was collected with a Whatman 542 Hardened Ashless filter paper. After ten runs, where a total of about 120 mg of simulant were used, the chamber was brought back to pressure. To determine precipitator efficiency, the dust adhering to the collector electrode was removed with running water that was passed through a second number 542 filter paper placed in a funnel above a flask being pumped slightly below atmospheric pressure to prevent overflowing. Crucibles containing the 542 filter papers were then placed in an oven at 550° Celisus until the paper burned off. Unused 543 filter papers were also placed in the oven as controls. Mass measurements of the precipitated and not collected dust yielded collection efficiencies ranging from 87 to 90%.

Since the size fraction of the sieved JSC Mars-1 simulant used contained particles larger than the under 10 μm fraction expected in the Martian atmosphere and since optical microscope images revealed that a large fraction of the particles that were not collected had diameters in the 30 to 70 μm range, we milled and sieved this simulant to obtain a more representative fraction. Experiments with this fine fraction yielded efficiencies of 94%.

It has been estimated that during a dust devil, there are about 10 particles per cubic centimeter.[11,12] However, the actual amount of dust that must be collected per unit time will also depend on the flow rate at which the ISRU gas intakes currently being designed will operate. This flow rate has been initially set at 88 g/h of CO_2. In the future, we will obtain upper flow rate limits yielding acceptable dust collecting efficiencies, those approaching 99%. These results may drive the designs of the gas intakes.

VI. Conclusion

Future human exploration of Mars will make use of local resources in the production of consumables and fuel. The Martian atmosphere, composed mostly of carbon dioxide, will be one of the most important resources for the production of oxygen and water. Before this extraction can take place, the ever present atmospheric dust must be removed. We have developed prototypes for an electrostatic precipitator technology that can remove dust from the Martian atmosphere. Experiments with a CO_2 atmosphere at 9 mbars of pressure have shown that, even with the limited potentials allowed by this low pressure, a controlled dust charging and dust collecting system can be implemented on Mars. The first prototype reaches dust collecting efficiencies of 94% for a relatively heavy atmospheric dust content. Although this dust content is higher than the estimated value of 10 particles per cubic centimeter during a dust devil, the actual amount of dust that must be removed will also depend on the flow at which the processing chambers, now in design, will operate.

Acknowledgments

This project was supported by NASA's In Situ Resource Utilization project.

References

[1]Townsend, J. S., *Electricity in Gases*, New York: Oxford University Press, 1914.

[2]Paschen, F., *Wied. Ann,* vol. 37, p. 69, 1889

[3]Calle, C.I. J. S. Clements, J. Willis and C. R. Buhler, "Paschen Breakdown Experiments in a Martian Atmosphere," *NASA Technical Memorandum 2004-211535,* pp.86-87, 2004.

[4]Kaiser, K.L., *Electromagnetic Compatibility Handbook,* Boca Raton: CRC Press, pp. 10-97, 2005.

[5]Calle, C.I., et al, "Electrostatic precipitation of dust in the Martian atmosphere: Implications for the utilization of resources during manned exploration missions," forthcoming, *J. Physics.*

[6]Landis, G.A. K. Herkenhoff, R. Greeley, S. Thompon, P. Whelley and the MER Athena Science Team, "Dust and Sand Deposition on the MER Solar Arrays as Viewed by the Microscopic Imager," *Lunar and Planetary Science,* vol. 37, p. 1937, 2006

[7]Romai, F.J. and D. Y. H. Piu, "On the Combination Coefficient of Positive Ions with Ultra-Fine Neutral Particles in the Transition and Free Molecular Regimes," *J. Aero. Sci.* vol. 23, pp. 679-692, 1993

[8]Filippov, A.V. "Charging of Aerosol in the Transition Regime," *J. Aerosol Science,* vol. 24, no. 4, pp. 424-436, 1993.

[9]Marlow, W.H. and J. R. Brock, "Unipolar Charging of Small Unipolar Particles," *J. Colloid Interface Science* vol. 50, pp. 32-38, 1975.

[10]Davison, S.W. and J. L. Gentry, "Difference in the Diffusion Charging of Dielectric and Conducting Ultra-Fine Aerosols," *Aerosol Sci. Tech.*, vol. 4, pp. 157-163, 1985

[11]Farrell, W.M. et al, "Detecting electrical activity from Martian dust storms," *J. Geophys. Res.*, 104, 3795-3801 (1999)

[12]Hviid, S.F. et al, "Magnetic properties experiments on the Mars Pathfinder lander: Preliminary results," *Science*, 278 1768 (1997)